Interface Tracking Simulation of Drops Rising Through Liquids in a Vertical Pipe Using Three Coordinate Systems

Hayashi, Kosuke
Kurimoto, Ryo
Tomiyama, Akio

(Citation)
The Journal of Computational Multiphase Flows,2(1):47-58

(Issue Date)
2010-03

(Resource Type)
journal article

(Version)
Accepted Manuscript

(URL)
https://hdl.handle.net/20.500.14094/90001608

Interface Tracking Simulation of Drops Rising Through Liquids in a Vertical Pipe Using Three Coordinate Systems

Kosuke Hayashi, Ryo Kurimoto and Akio Tomiyama
Graduate School of Engineering, Kobe University
1-1, Rokkodai, Nada, Kobe, 657-8501, Japan
e-mail:tomiyama@mech.kobe-u.ac.jp

[Received date; Accepted date] – to be inserted later

Abstract
Interface tracking simulations of single drops rising through a vertical pipe are carried out using three coordinate systems, i.e. cylindrical, general curvilinear and Cartesian coordinates, to investigate the effects of coordinate system and spatial resolution on the accuracy of predictions. Experiments of single drops in a vertical pipe are also conducted to obtain experimental data for comparisons with simulations. The drop shape observed are spheroidal and deformed spheroidal at low values of the diameter ratio, λ, of the sphere-volume equivalent diameter of a drop to the pipe diameter, whereas they take bullet-shapes at large λ. The conclusions obtained are as follows: (1) the effects of coordinate system on drop shape are small at low λ. At large λ, the effects are also small for drops in a low viscosity system, whereas non-physical shape distortion takes place when the Cartesian coordinates are used with low spatial resolution for drops in a high viscosity system, and (2) the drop terminal velocity and the velocity profile in the liquid film between a bullet-shaped drop and a pipe wall are well predicted using all the coordinate systems tested even at low spatial resolution.

Keywords: Interface Tracking Method, Cylindrical Coordinates, Curvilinear Coordinates, Cartesian coordinates, Drop.

1. INTRODUCTION

Interface tracking simulations based on a volume-of-fluid (VOF) method [1] now play an important role in modeling two-phase flows [2-4]. VOF methods based on Cartesian coordinates have been widely used to simulate two-phase flows in simple geometries such as bubbles and drops in infinite media, sloshing in a rectangular tank and so on. However, when simulating flows in practical systems such as oil transportation pipelines, rod bundles in a boiling water reactor and so on, it would be desirable for VOF to possess the ability of dealing with curvilinear coordinates. For example, it may be taken for granted that flows in a pipe are best simulated using cylindrical and general curvilinear coordinates, because the circular cross-section of the pipe is correctly represented by these coordinate systems as shown in Figs. 1 (a) and (b). On the other hand, the circular pipe wall may be represented by jaggy boundary as shown in Fig. 1 (c) when Cartesian coordinate system is used. Several VOF methods based on curvilinear coordinates have been, therefore, developed [5, 6].

The authors also developed a VOF method called NSS (Non-uniform Subcell Scheme) [7], which can deal with three coordinate systems, i.e. three-dimensional Cartesian, general curvilinear and cylindrical coordinates [7, 8]. The accuracy of NSS has been examined for several dispersed two-phase flows. The examination has demonstrated that (1) NSS based on Cartesian coordinates gives good predictions for shapes and terminal velocities of bubbles and drops in infinite stagnant liquids [7], (2) terminal velocities and shapes of bubbles flowing in a two by two rod bundle are well predicted by making use of the general curvilinear coordinates [8], and (3) an air bubble

flowing in a laminar water flow in a vertical pipe is reasonably predicted using cylindrical coordinates [8].

Though the curvilinear coordinate systems can correctly represent curved boundaries, it is not an easy task to generate appropriate grids for the whole computational domain for a highly complicated flow geometry. In that case, Cartesian coordinates may be still useful from a practical point of view, provided that the error due to the jaggy representation of complicated geometry is not large. Hence it is important to know the effects of coordinate system on the accuracy of predictions. Tomiyama et al. [9] and Yoshida et al. [10] carried out VOF simulations based on Cartesian coordinates for a Taylor bubble in a vertical pipe and large bubbles in a two by two rod bundle, respectively. In spite of the jaggy representation of the walls, they could obtain good predictions for the bubble terminal velocities, that is, the jaggy boundary does not have much influence on the accuracy of the predicted terminal velocity for the cases of rising air bubbles in stagnant water. In contrast to bubbles in low viscosity system, accurate evaluation of wall friction is more important to obtain good predictions of drops moving through viscous liquids at low drop Reynolds numbers. Hence, the error in the evaluation of wall friction due to the jaggy boundary might strongly affect the motions of drops in liquids. However, the effects of the jaggy boundary on the motions of drops have not been investigated yet.

In this study, interface tracking simulations of single drops rising through stagnant liquids in a vertical pipe are, therefore, carried out using the three different coordinate systems, i.e. cylindrical, general curvilinear and Cartesian coordinates, to investigate the effects of coordinate system on the drop velocity and shape. The errors in the velocity and shape due to the jaggy boundary may depend on spatial resolution. Hence, we also investigate the effects of spatial resolution on predicted drop velocities and shapes. Experiments of single drops in a vertical pipe are also carried out to obtain experimental data for comparisons with simulations.

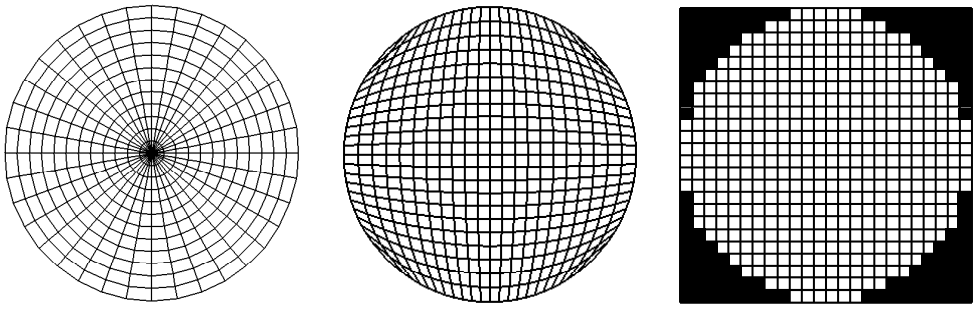

(a) Cylindrical coordinates (b) General curvilinear coordinates (c) Cartesian coordinates

Fig. 1 Cross-sectional views of computational grids for circular pipe

2. NUMERICAL METHOD

The continuity and momentum equations based on the one-field approximation [1, 4] are given by

$$\nabla \cdot \boldsymbol{u} = 0 \tag{1}$$

$$\frac{\partial \boldsymbol{u}}{\partial t} + \boldsymbol{u} \cdot \nabla \boldsymbol{u} = -\frac{\nabla P}{\rho} + \frac{1}{\rho} \nabla \cdot \mu [\nabla \boldsymbol{u} + (\nabla \boldsymbol{u})^{\mathrm{T}}] + \boldsymbol{g} + \frac{\sigma K \boldsymbol{n} \delta}{\rho} \tag{2}$$

where $\boldsymbol{u}$ is the velocity, t the time, P the pressure, ρ the mixture density, μ the mixture viscosity, $\boldsymbol{g}$ the acceleration of gravity, σ the surface tension, K the mean curvature, δ the delta function which is non-zero only at the interface, $\boldsymbol{n}$ the unit normal to the interface, and the superscript T denotes the transpose. The density and viscosity are given by

$$\rho = \rho_C \alpha + \rho_D (1 - \alpha) \tag{3}$$

$$\frac{1}{\mu} = \frac{\alpha}{\mu_C} + \frac{1-\alpha}{\mu_D} \tag{4}$$

where α ($0 < \alpha < 1$) is the cell-averaged volume fraction of the continuous phase and the subscripts C and D denote the continuous and dispersed phases, respectively. The interface lies in computational cells in which $0 < \alpha < 1$.

The interface is tracked by solving the following advection equation:

$$\frac{\partial \alpha}{\partial t} + \nabla \cdot \alpha \boldsymbol{u} = \alpha \nabla \cdot \boldsymbol{u} \tag{5}$$

An interface tracking method based on a non-uniform subcell scheme (NSS) was proposed in our previous study [7] to accurately solve eqns. (1)-(5). The amount of fluid volumes transferred from an interface cell to its neighbor cells is accurately calculated by making use of non-uniform subcells which are temporarily introduced only in interface cells. A local distance function is also computed in interface cells, by which the surface tension force is accurately evaluated. NSS can deal with not only Cartesian coordinates but also cylindrical and general curvilinear coordinates. A detailed description of the extension to cylindrical and general curvilinear coordinate systems can be found in Ref. [8].

3. EXPERIMENTAL SETUP AND CONDITIONS

Measurements of shapes and terminal velocities of single drops rising through stagnant liquids in a vertical pipe were carried out to obtain experimental data for comparisons with simulations. Figure 2 shows the experimental setup. The experimental apparatus is the same as that used in our previous study [3]. The vertical pipe and the lower and upper tanks were made of transparent acrylic resin. The length and inner diameter, D, of the pipe were 530 and 20.1 mm, respectively. Silicon oil (Sinetsu Silicon, KF96-30) and glycerol-water solutions were used for drops and the continuous phase, respectively. A small amount of silicon oil was stored in the hemispherical glass cup. A single drop was released by rotating the cup. An image processing method [11] was used to evaluate drop diameters and velocities from drop images taken by using a high-speed video camera (Redlake, HS-1, frame rate 400 frame/s) at 350 mm above the bottom of the pipe. All the measured drops reached their terminal conditions at this elevation. The pipe was enclosed with the acrylic duct. The gap between the pipe and the duct was filled with the same glycerol-water solution as that in the pipe to reduce optical distortion of drop images. A LED light source (Hayashi Watch-Works, LP-2820) was used for backward illumination. The glycerol concentration was set at 85.3% and 74.0% to carry out comparisons with simulations for two fluid systems. The fluid properties are summarized in Table 1. The dimensionless numbers, M and κ, in Table 1 are the Morton number and the viscosity ratio, respectively. They are defined by

$$M = \frac{g \mu_C^4 (\rho_C - \rho_D)}{\rho_C^2 \sigma^3} \tag{6}$$

$$\kappa = \frac{\mu_D}{\mu_C} \tag{7}$$

where g is the magnitude of the acceleration of gravity. The experiments were carried out for $0.1 < \lambda < 1.1$ where λ is the diameter ratio defined by

$$\lambda = \frac{d}{D} \tag{8}$$

Here d is the sphere-volume equivalent diameter of a drop.

4. TEST CONDITIONS

Simulations were carried out under the same conditions as experiments. The diameter ratios simulated were $\lambda \sim 0.3$, 0.5 and 1.0. Figure 3 shows an example of cylindrical grids for $\lambda \sim 0.5$ and $d^* = 9$, where d^* is the number of computational cells assigned to the drop diameter d. For $\lambda \sim 0.3$ and 0.5, no-slip condition was imposed on the side and bottom boundaries. The top boundary was continuous outflow. A spherical drop of diameter d was initially placed near the bottom boundary. The pipe length was $7d$. When simulating large drops of $\lambda \sim 1.0$, the boundary conditions for the top and bottom boundaries were inflow and outflow, respectively, and that of the side boundary was a wall moving downward at the drop terminal velocity, V_T. The pipe length was $5d$. The initial drop shape was a cylinder with two hemispheres attached to the top and bottom of the cylinder.

The effects of spatial resolution were examined by changing d^*. The values of d^* tested were 6, 9 and 12 for drops of $\lambda < 0.5$, and 12 and 24 for drops of $\lambda \sim 1.0$. Figure 4 shows examples of cross-sectional view of the computational grids.

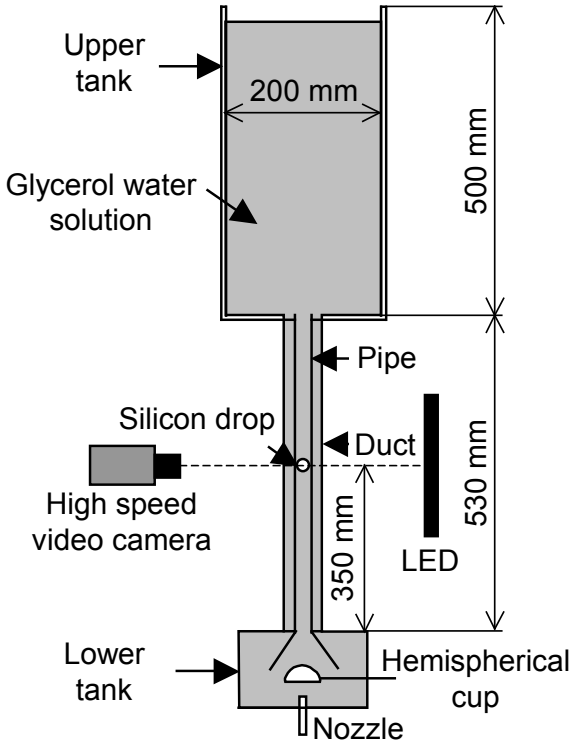

Fig. 2 Experimental setup

Table. 1 Experimental conditions (temperature: 25 ± 0.5 °C)

log$M$	κ	ρ_C [kg/m^3]	ρ_D [kg/m^3]	μ_C [mPa·s]	μ_D [mPa·s]	σ [mN/m]	Glycerol concentration [%]
–2.5	0.34	1220	955	85.3	28.7	31.0	85.3
–4.7	1.1	1190	955	25.2	28.7	32.3	74.0

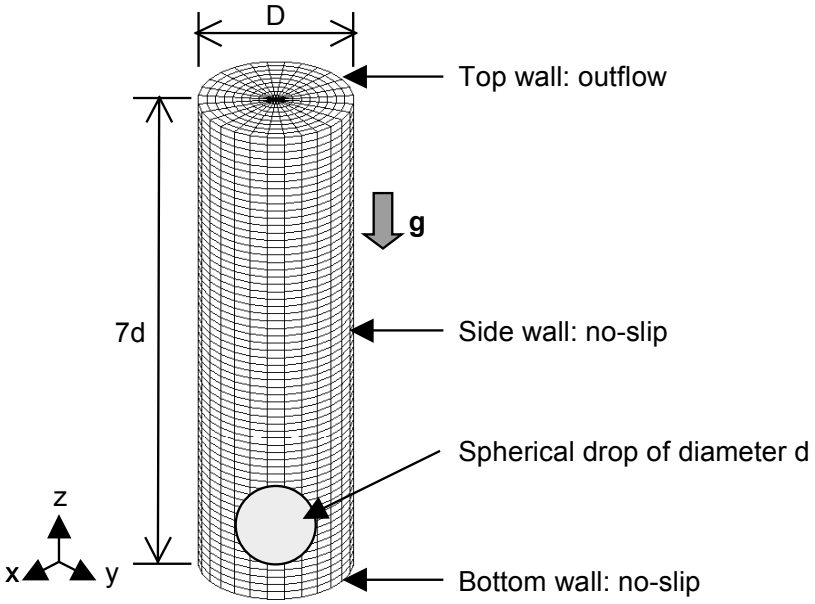

Fig. 3 Computational domain for $\lambda \sim 0.5$ and $d^* = 9$

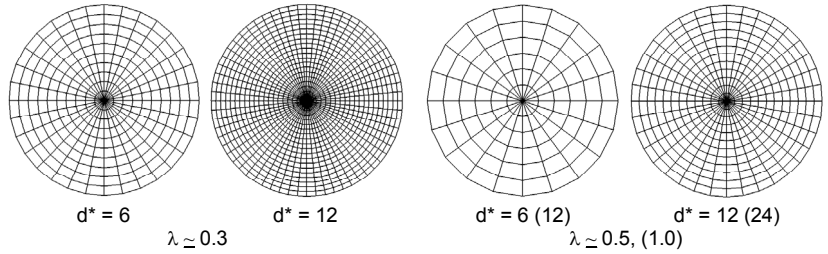

(a) Cylindrical grid

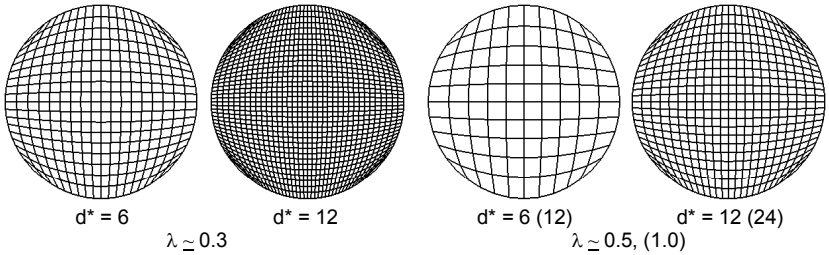

(b) Curvilinear grid

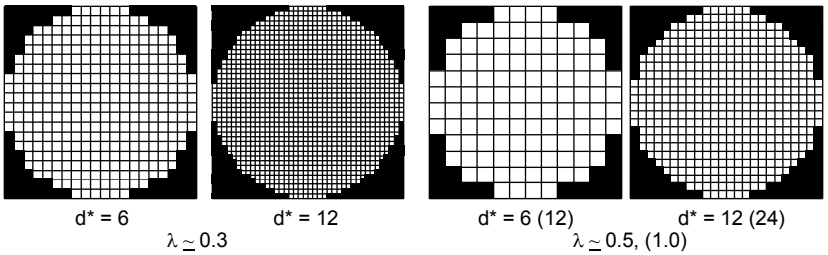

(c) Cartesian grid

Fig. 4 Computational grids used in simulations

5. RESULTS AND DISCUSSION

Measured terminal velocities of drops are plotted against the diameter ratio in Fig. 5. The data for $\lambda < 0.6$ were obtained in the previous study [3]. The terminal velocity can be classified into three regimes: regime I in which V_T increases with λ, regime II in which V_T decreases with increasing λ and regime III where V_T is independent of λ. In regime I, the effects of pipe wall on drop shape and V_T are not significant and the main characteristic length governing the velocity of drops is the drop diameter, d [3]. As shown in Fig. 6 (a), drop shapes in regime I are spheroidal. In regime II, the wall effect is much stronger than that in regime I. Drops do not have the fore-aft symmetry due to the strong wall effect as shown in Fig. 6 (b). Drops in regime III are shown in Fig. 6 (c). The drop in this regime is composed of a round nose and a cylindrical section surrounded by an annular liquid film. These drops can be called Taylor drops and the characteristic length governing the terminal velocity of Taylor drops is the pipe diameter, D [12, 13]. The rear shape of the Taylor drop at log$M$ = –2.5 is oblate spheroidal, while the Taylor drop in the lower viscosity system (log$M$ = –4.7) is associated with a wave disturbance at the rear end [14].

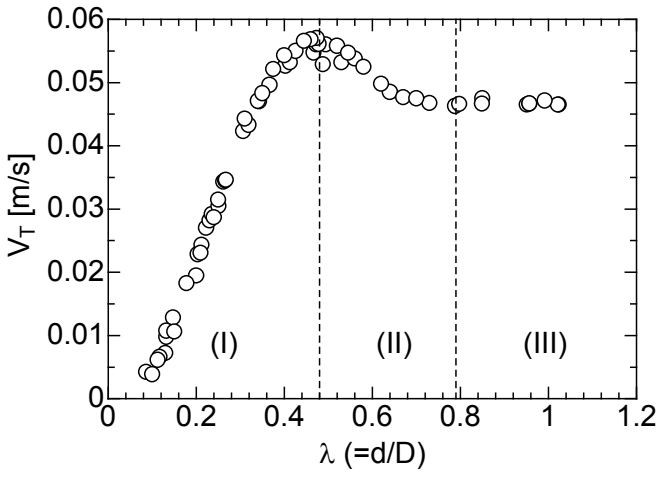

(a) log$M$ = –2.5

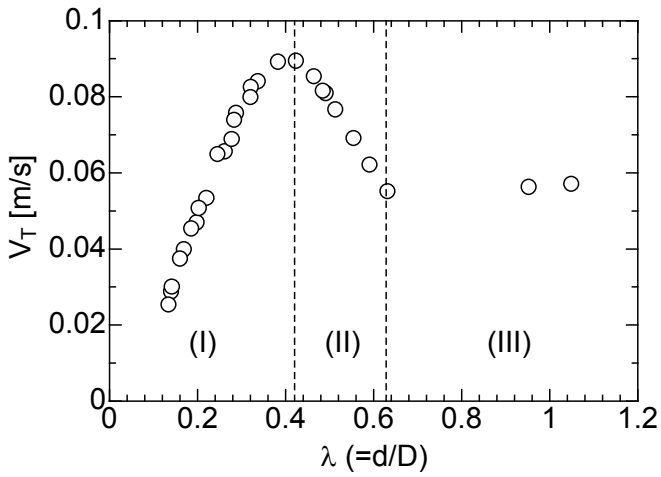

(b) log$M$ = –4.7

Fig. 5 Terminal velocities of single drops in the vertical pipe, D = 20.1 mm

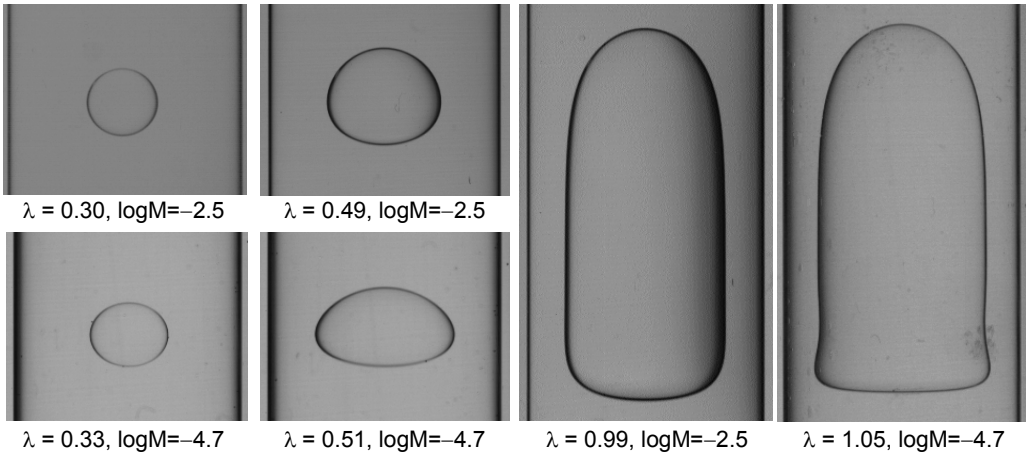

Fig. 6 Drop shapes in regimes I ($\lambda \simeq 0.3$), II ($\lambda \simeq 0.5$) and III ($\lambda \simeq 1.0$)

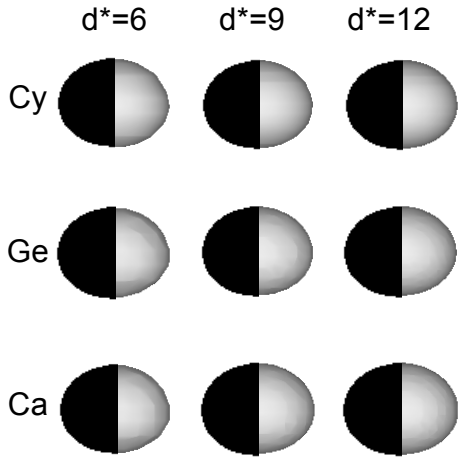

Fig. 7 Shapes of drops in regime I at $\lambda = 0.33$ and log$M = -4.7$
(left: measured, right: predicted)

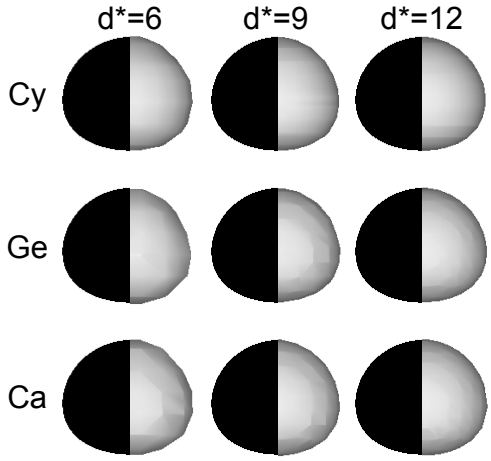

Fig. 8 Shapes of drops in regime II at $\lambda = 0.49$ and log$M = -2.5$
(left: measured, right: predicted)

Figure 7 shows comparisons between measured and predicted drop shapes in regime I at log$M$ = –4.7, in which Cy, Ge and Ca denote cylindrical, general curvilinear and Cartesian coordinates, respectively. The drop shapes are well predicted for all the coordinate systems and d*. Hence the coordinate system and the spatial resolution do not have much influence on the accuracy of simulation. Drop shapes in regime II at log$M$ = –2.5 are shown in Fig. 8. The predicted shapes also agree with the measured shapes for all the coordinate systems and d*. Figure 9 (a) shows Taylor drops at log$M$ = –2.5. The shapes predicted with d* = 24 are in good agreement with the measured ones, and do not depend on the coordinate system. The dependency becomes clear in the results at d* = 12. The difference between the predictions of d* = 24 and 12 is not significant when the cylindrical and general curvilinear coordinates are used, whereas in the Cartesian coordinates non-physical distortion appears in the vicinity of the border between the round nose and the cylindrical section of the Taylor drop at d* = 12 and the predicted length of the drop increases as d* decreases. At log$M$ = –4.7, the effect of the coordinate system is not significant even at d* = 12 as shown in Fig. 9 (b). The rear shape of the cylindrical section is, however, completely different from the measured shape at d* = 12 due to the insufficient spatial resolution. On the other hand, the wave disturbance at the rear end is reproduced at the high spatial resolution, d* = 24, in all the coordinate systems.

Comparison of the velocity profile in the radial direction at the cylindrical part of the Taylor drop at d* = 24 is shown in Fig. 10 (a). The broken lines represent the interface location. Only a few computational cells, i.e. four cells in the Cylindrical and Cartesian coordinates and three cells in the curvilinear coordinates, lie in the liquid film. The predictions obtained using the cylindrical and curvilinear coordinates are in very good agreement. In spite of the jaggy representation of the pipe wall, the Cartesian coordinates also give the same velocity profile as the other coordinate systems. Figure 10 (b) shows the velocity profiles at d* = 12. The number of cells in the liquid film is only two in the cylindrical and Cartesian coordinates, and is only one in the curvilinear coordinates. Though the velocity profiles at d* = 12 are different from those at d* = 24 for all the coordinate systems, they are qualitatively reasonable.

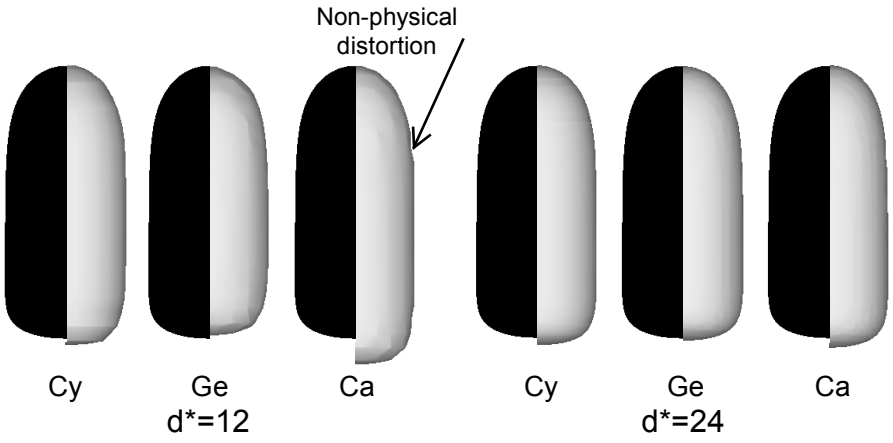

(a) λ = 0.99, log$M$ = –2.5

Fig. 9 Shapes of drops in regime III ($\lambda \simeq 1.0$, left: measured, right: predicted)

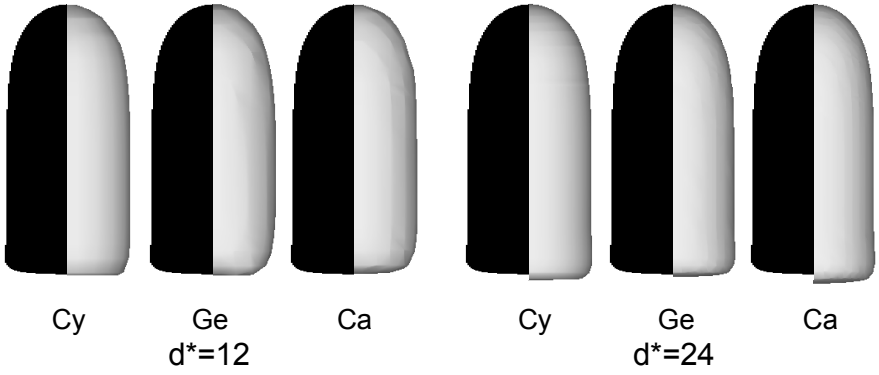

(b) λ = 1.05, log$M$ = –4.7

Fig. 9 Contd.

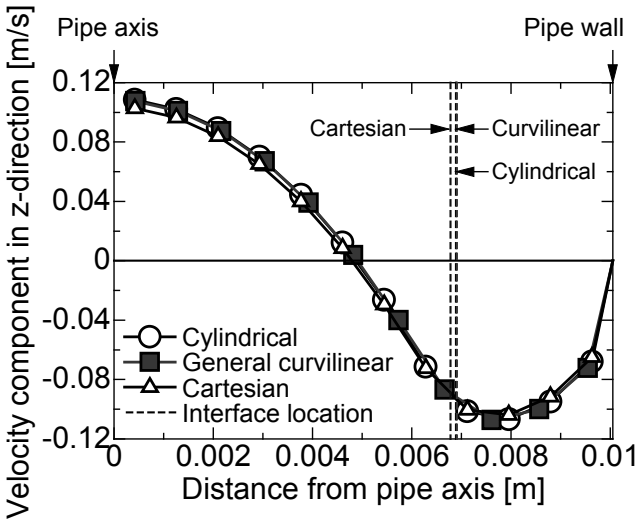

(a) d^* = 24

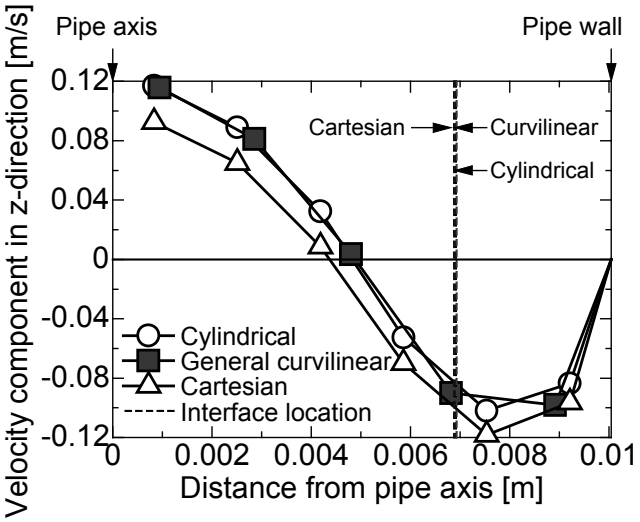

(b) d^* = 12

Fig. 10 Velocity profile in the radial direction at cylindrical part of Taylor drop
(λ = 0.99, log$M$=–2.5)

Comparisons between measured and predicted terminal velocities are shown in Fig. 11. The spatial resolutions are $d^* = 12$ for the drops in regimes I and II, and 24 for the drops in regime III. For all the cases, the predictions are in good agreement with the experimental data, that is, the coordinate system do not have much influence on V_T in all the regimes. Figure 12 shows predicted V_T obtained by changing d^*. The effect of d^* on V_T is also not significant. The maximum deviation, $[V_T(\text{high } d^*) - V_T(\text{low } d^*)]/V_T(\text{high } d^*)$, is 6.2 %.

The effects of coordinate system on shape and terminal velocity of a drop are very small in regimes I and II. Though non-physical shape distortion takes place when the Cartesian coordinate system is used with low spatial resolution for Taylor drops in a high viscosity system, the drop terminal velocity can be well predicted. Hence, the Cartesian coordinates can be used to obtain reasonable predictions of shapes and velocities for drops rising through stagnant liquids in a vertical pipe, provided that the spatial resolution d^* is larger than 6 for regime I and II and 12 for regime III.

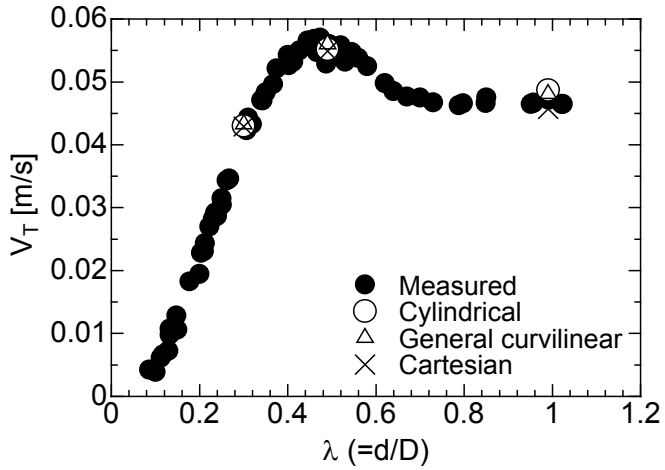

(a) log$M$ = –2.5

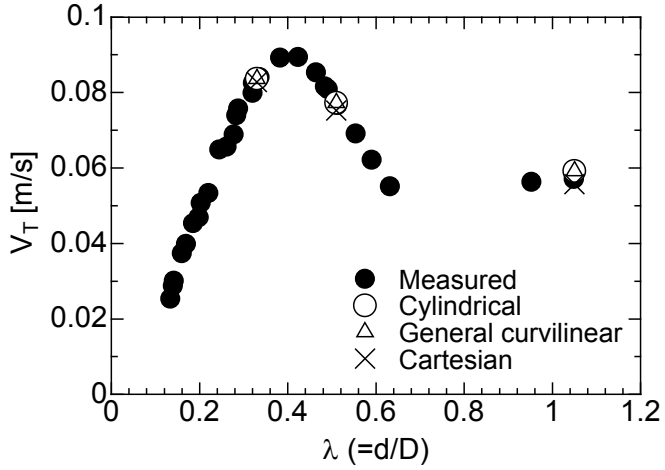

(b) log$M$ = –4.7

Fig. 11 Comparisons of terminal velocities between measurements and predictions

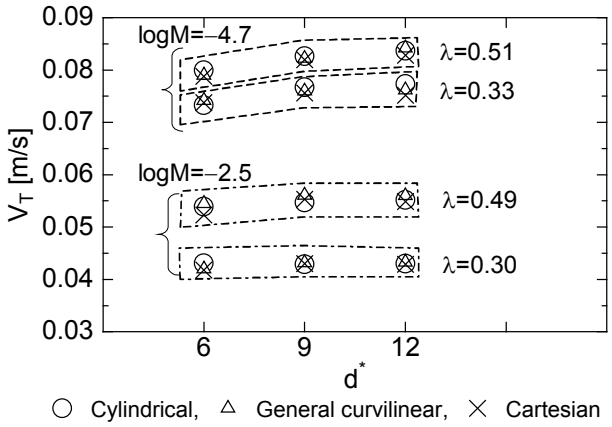

(a) λ ~ 0.3 and 0.5

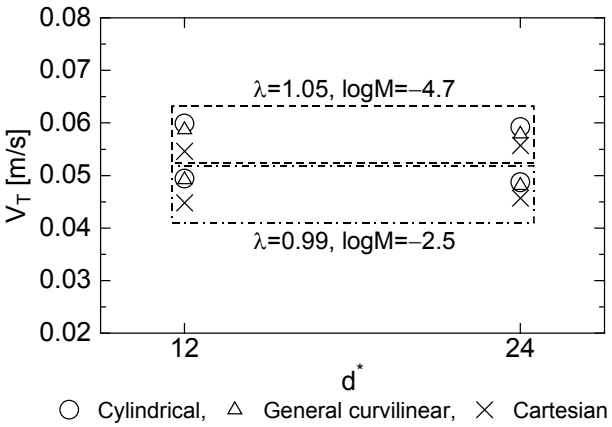

(b) λ ~ 1.0

Fig. 12 Dependence of terminal velocity on *d**

6. CONCLUSIONS

Interface tracking simulations of drops rising through a vertical pipe were carried out using three coordinate systems to investigate the effects of coordinate system and spatial resolution on the accuracy of predictions. The coordinate systems tested were the cylindrical, general curvilinear and Cartesian coordinate systems. Experiments of single rising drops in the pipe were also conducted to obtain the experimental data for comparisons with the simulations. The measured terminal velocity V_T was classified into the three regimes: regime I in which V_T increases with the diameter ratio λ, regime II in which V_T decreases as increasing λ and regime III where V_T is independent of λ. The drop shapes in regimes I, II and III were spheroidal, deformed spheroidal and bullet-shape (Taylor drop), respectively. The simulations were carried out for these three regimes. The following conclusions were obtained:

(1) The effects of coordinate system on drop shape are small for drops in regimes I and II. In regime III, the effects are also small for drops in a low viscosity system, whereas non-physical shape distortion takes place when the Cartesian coordinates are used with low spatial resolution for drops in a high viscosity system.

(2) The drop terminal velocity and the velocity profile in the liquid film between a Taylor drop and a pipe wall are well predicted using all the coordinate systems even at low spatial resolution.

ACKNOWLEDGEMENTS

This work has been supported by the Japan Society for the Promotion of Science (grant-in-aid for scientific research (B), No. 21360084). The authors would like to express our thanks to Mr. Keishun Hirokawa and Mr. Yasuki Yoshikawa for their great help in the experiment.

REFERENCES

[1] Hirt, C. W., and Nicholds, B. D., Volume of Fluid (VOF) Method for the Dynamics of Free Boundaries, *Journal of Computational Physics*, 1981, 39, 201-225.

[2] Simcik, M., Ruzicka, M.C., and Drahos, J., Computing the Added Mass of Dispersed Particles, *Chemical Engineering Science*, 2008, 63, 4580-4595.

[3] Hayashi, K. and Tomiyama, A., A Drag Correlation of Fluid Particles Rising through Stagnant Liquids in Vertical Pipes at Intermediate Reynolds Numbers, *Chemical Engineering Science*, 2009, 64, 3019-3028.

[4] Scardovelli, R. and Zaleski, S., Direct Numerical Simulation of Free-Surface and Interfacial Flow, *Annual Review of Fluid Mechanics*, 1999, 31, 567-603.

[5] Himeno, T. and Watanabe, T., Thermo-Fluid Management under Low-gravity Conditions (2nd Report, Free-Surface Flows Driven by Surface Forces), *Transaction of Japanese Society of Mechanical Engineers, Series B*, 2003, 69(687), 2400-2407. *(in Japanese)*

[6] Jang, W., Jilesen, J., Lien, F. S. and Ji, H., A Study on the Extension of a VOF/PLIC based Method to a Curvilinear Co-ordinate, *International Journal of computational Fluid Dynamics*, 2008, 22(4), 241-257.

[7] Hayashi, K., Sou, A. and Tomiyama, A., A Volume Tracking Method based on Non-Uniform Subcells and Continuum Surface Force Model using a Local Level Set Function, *Computational Fluid Dynamics Journal*, 2006, 15, 225-232.

[8] Hayashi, K. and Tomiyama, A., Interface Tracking Simulation of Bubbles and Drops in Complex Geometries, *Multiphase Science and Technologies*, 2007, 19, 121-140.

[9] Tomiyama, A., Nakahara, Y. and Hosokawa, S., An Interface Tracking Method based on Volume Tracking in Micro Cells Embedded in Regular Computational Cells, *Computational Fluid Dynamics Journal*, 2003, 11(4), 411-419.

[10] Yoshida, H., Ose, Y., Kureta, M., Nagayoshi, T., Takase, K. and Akimoto, H., Investigation of Water-Vapor Two-Phase Flow Characteristics in a Tight-Lattice Core by Large-Scale Numerical Simulation (IV), *Transaction of Atomic Energy Society of Japan*, 2005, 4(2), 106-114. (*in Japanese*)

[11] Tomiyama, A., Celata, G. P., Hosokawa, S. and Yoshida, S., Terminal Velocity of Single Bubbles in Surface Tension Force Dominant Regimem, *International Journal of Multiphase Flow*, 2002, 28(9), 1497-1519.

[12] Clift, R., Grace, J. R. and Weber, M. E., *Bubbles, Drops, and Particles*, Academic Press, 1978.

[13] Wallis, G. B., *One-Dimensional Two-phase Flow*, McGraw Hill, 1969.

[14] Goldsmith, H. L. and Mason, S. G., The Movement of Single Large Bubbles in Closed Vertical Tubes, *Journal of Fluid Mechanics*, 1962, 14, 42-58.

NOMENCLATURE

d	sphere-volume equivalent diameter of a drop [m]
d^*	the number of computational cells assigned to drop diameter d
D	pipe diameter [m]
g	magnitude of the acceleration of gravity [m/s^2]
$\boldsymbol{g}$	acceleration of gravity [m/s^2]
K	mean curvature [m^{-1}]
M	Morton number ($=g\mu_C^4(\rho_C - \rho_D)/\rho_C^2\sigma^3$)
$\boldsymbol{n}$	unit normal to the interface
P	pressure [Pa]
t	time [s]
$\boldsymbol{u}$	velocity [m/s]
V_T	terminal velocity [m/s]
α	cell-averaged volume fraction of the continuous phase

δ	delta function
κ	viscosity ratio ($=\mu_D/\mu_C$)
λ	diameter ratio ($=d/D$)
μ	mixture viscosity [Pa·s]
μ_D	viscosity of dispersed phase [Pa·s]
μ_C	viscosity of continuous phase [Pa·s]
ρ	mixture density [kg/m^3]
ρ_D	density of dispersed phase [kg/m^3]
ρ_C	density of continuous phase [kg/m^3]
σ	surface tension [N/m]